communications biology

Article

https://doi.org/10.1038/s42003-024-07028-1

RABIF promotes hepatocellular carcinoma progression through regulation of mitophagy and glycolysis

Ning Feng[1,5], Rui Zhang[1,5], Xin Wen[1,2], Wei Wang[1], Nie Zhang[1], Junnian Zheng[1,3], Longzhen Zhang[2,3] ✉ & Nianli Liu[1,3,4] ✉

The RAB interacting factor (RABIF) is a putative guanine nucleotide exchange factor that also functions as a RAB-stabilizing holdase chaperone. It has been implicated in pathogenesis of several cancers. However, the functional role and molecular mechanism of RABIF in hepatocellular carcinoma (HCC) are not entirely known. Here, we demonstrate an upregulation of RABIF in patients with HCC, correlating with a poor prognosis. RABIF inhibition results in decreased HCC cell growth both in vitro and in vivo. Our study reveals that depleting RABIF attenuates the STOML2-PARL-PGAM5 axis-mediated mitophagy. Consequently, this reduction in mitophagy results in diminished mitochondrial reactive oxygen species (mitoROS) production, thereby alleviating the HIF1α-mediated downregulation of glycolytic genes HK1, HKDC1, and LDHB. Additionally, we illustrate that RABIF regulates glucose uptake by controlling RAB10 expression. Importantly, the knockout of RABIF or blockade of mitophagy sensitizes HCC cells to sorafenib. This study uncovers a previously unrecognized role of RABIF crucial for HCC growth and identifies it as a potential therapeutic target.

Hepatocellular carcinoma (HCC) is the sixth most common human cancer and fourth leading cause of cancer-related mortality, with an annual rise worldwide[1]. Although several targeted therapies have been developed for the treatment of HCC, the prognosis is still poor due to therapy resistance and a high rate of recurrence[2]. Hence, there is a pressing imperative to pinpoint innovative molecular targets and unravel the underlying mechanisms, fostering the advancement of novel and efficacious therapeutic approaches.

Hepatocytes exhibit a strong regenerative capacity and demand elevated levels of energy. It has been shown that metabolic reprograming is an important feature of HCC[3]. Mitochondria are the central organelles of cells, which play an essential role in cellular metabolism by producing ATP via the oxidative phosphorylation (OXPHOS) pathway. Numerous reports indicate that a substantial number of hepatocellular carcinoma cells possess malfunctioning mitochondria, suggesting their reliance on mitochondrial function and a potential association with mitochondrial abnormalities[4,5]. Mitophagy is a crucial process orchestrated by a pathway involving the PINK1 kinase and the PARKIN ubiquitin ligase, selectively removes malfunctioning mitochondria to preserve a functional mitochondrial network in tumor cells. The breakdown products of these dysfunctional mitochondria can be further utilized as bioenergetic intermediates to sustain unlimiting growth[6]. Mitophagy has been implicated in various cancer types, including HCC[7–9].

The RAB GTPase family consists of more than 60 members, is the largest branch of the Ras superfamily to date[10], and plays a pivotal role in regulating vesicular transport, membrane trafficking, and fusion[11–13]. It has been well documented that RAB proteins are involved in mitophagy pathway[14]. For example, one study has reported that RAB7 is involved in mitophagosome formation in Parkin-mediated mitophagy[15]. Some other RAB proteins such as RAB8A, RAB8B, and RAB13 were found to be phosphorylated by PINK1 and function as downstream effectors of PINK1[16].

RAB proteins are activated by guanine exchange factors (GEFs) in the GTP-bound state. RABIF was one of the first putative RAB GEFs identified[17]. It binds to a subset of secretory RAB proteins (Rab1b, Rab3a, Rab8a, Rab10, Rab12, Rab13 and Rab18) and possesses GEF activity towards Rab1, Rab3a, and Rab8a[18]. Recent studies indicate that RABIF functions as a holdase chaperone rather than a GEF[19,20]. Several RABIF-interacting RAB proteins have been found play important roles in HCC[21,22], suggesting that RABIF may be involved in liver cancer development.

[1]Cancer Institute, Xuzhou Medical University, Xuzhou, Jiangsu, China. [2]Department of Radiation Oncology, Affiliated Hospital of Xuzhou Medical University, Xuzhou, Jiangsu, China. [3]Center of Clinical Oncology, Affiliated Hospital of Xuzhou Medical University, Xuzhou, Jiangsu, China. [4]Department of Pathology and Laboratory of Medicine, Tulane University, New Orleans, LA, USA. [5]These authors contributed equally: Ning Feng, Rui Zhang. ✉e-mail: jsxyfyzlz1@163.com; liunli@xzhmu.edu.cn

However, the role and underlying mechanisms of RABIF in HCC progression remain to be investigated.

Sorafenib, a multi-target tyrosine kinase inhibitor (TKI), demonstrates antiangiogenesis and antiproliferation effects, extending median survival in advanced HCC patients from 7.9 to 10.7 months[23]. As the FDA-approved first-line therapy for advanced HCC, sorafenib initially shows promise, but nearly all patients develop resistance within a few months. Recent studies indicate that epigenetics, transport processes, regulated cell death, and the tumor microenvironment play roles in the initiation and development of sorafenib resistance in HCC[24]. Understanding these molecular mechanisms is essential to identifying new therapeutic targets and improving outcomes for HCC patients.

The present study is designed to explore the functions and underlying mechanisms of RABIF in HCC. We found that RABIF was overexpressed in HCC and was inversely correlated with the prognosis of HCC patients. We further demonstrated that RABIF promotes HCC cell growth both in vitro and in vivo. Mechanistic studies indicated that RABIF resides in the mitochondria and interacts with STOML2. Depletion of RABIF suppressed STOML2-PARL-PGAM5 axis-mediated mitophagy, which in turn reduced mtROS production and HIF1α-dependent glycolytic gene expression. Our results also revealed that RABIF regulated glucose uptake by controlling RAB10 expression. In addition, we found that depletion of RABIF or suppression of mitophagy can overcome sorafenib resistance in HCC, which may provide a novel strategy to improve the therapeutic efficacy of sorafenib in HCC patients.

Results

RABIF is upregulated in HCC and predicts poor prognosis

To test the RABIF dependency of HCC, we first evaluated the expression pattern of RABIF across cancers using data from the Cbioportal datasets. Our analysis showed that RABIF is amplified in several types of cancers, particularly in 8% of breast cancers and 6% of liver cancers (Fig. 1A). Similarly, the amplified RABIF gene was observed in an HCC patient-derived xenograft (PDX) cohort from PDXliver (Fig. 1B). Copy number amplification of RABIF was significantly correlated with its mRNA expression (Fig. 1C). We observed elevated RABIF expression in both unpaired and paired HCC tissues from the TCGA datasets (Fig. 1D and E). RABIF expression was also significantly upregulated at each pathological stage of HCC compared to normal tissues (Fig. 1F). Moreover, in silico analysis of two independent datasets from GEO revealed that RABIF expression was upregulated in HCC tissues compared with that in normal tissues (Fig. 1G). To further confirm the expression of RABIF in HCC, we

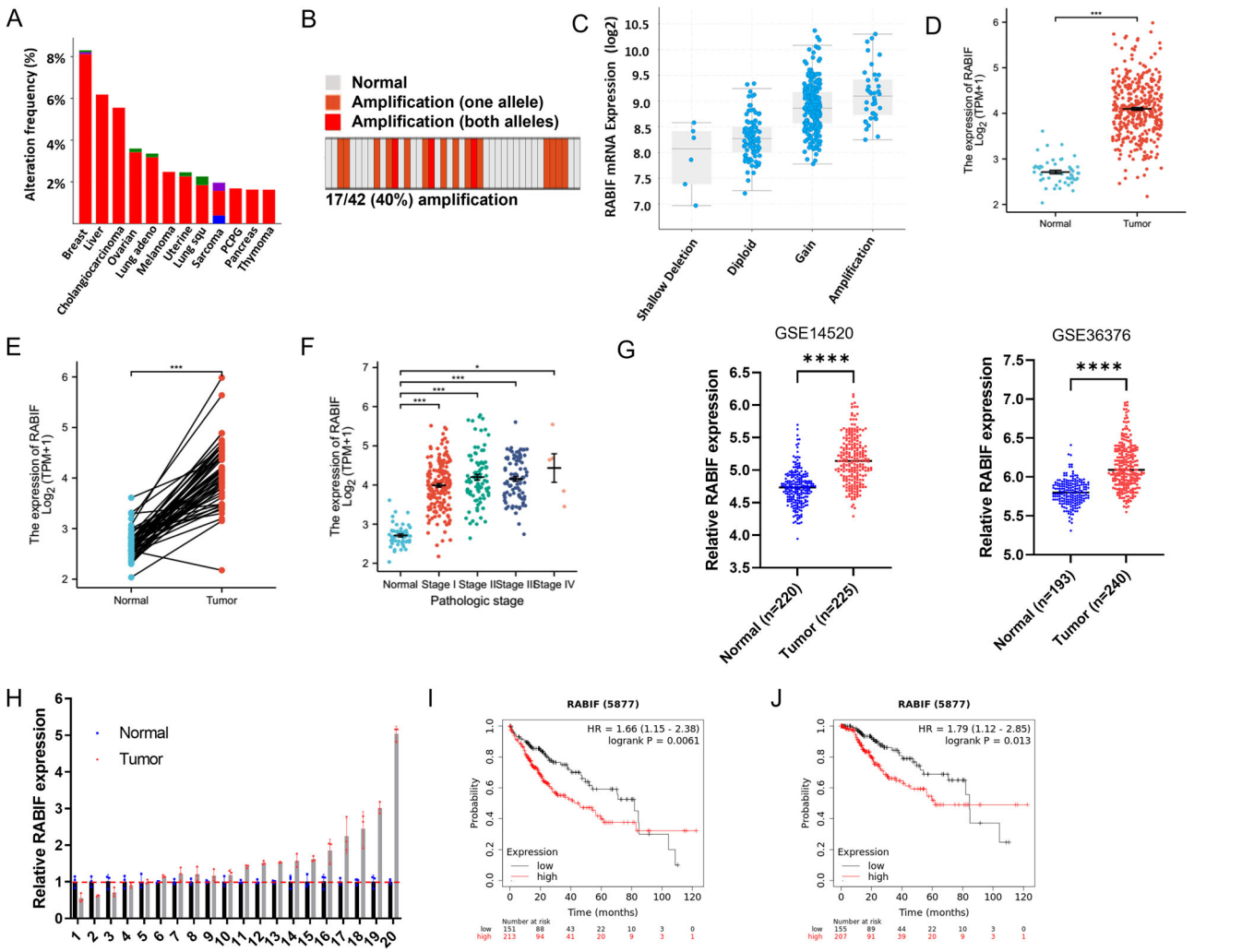

Fig. 1 | RABIF upregulation correlates with poor prognosis in HCC. A cBioportal examination of TCGA databases revealed RABIF genomic changes in human malignancies. **B** RABIF amplification in HCC PDX. **C** RABIF expression levels are positively linked to gene copy counts. **D, E** RABIF expression was compared in HCC to nonmatched (**D**) and matched (**E**) normal tissues. **F** RABIF expression levels are upregulated in each HCC pathologic stage. **G** The expression of RABIF in HCC tissues and normal tissues was examined based on GSE14520 and GSE36376 datasets. **H** RABIF expression in cDNA array containing 20 pairs of liver tissue was determined by RT-qPCR. **I, J** Correlation between RABIF expression and overall survival (**I**) as well as disease-free survival (**J**) was analyzed by Kaplan−Meier Plotter (http://www.kmplot.com/analysis/). $^{*}p < 0.05$, $^{**}p < 0.01$, $^{***}p < 0.001$.

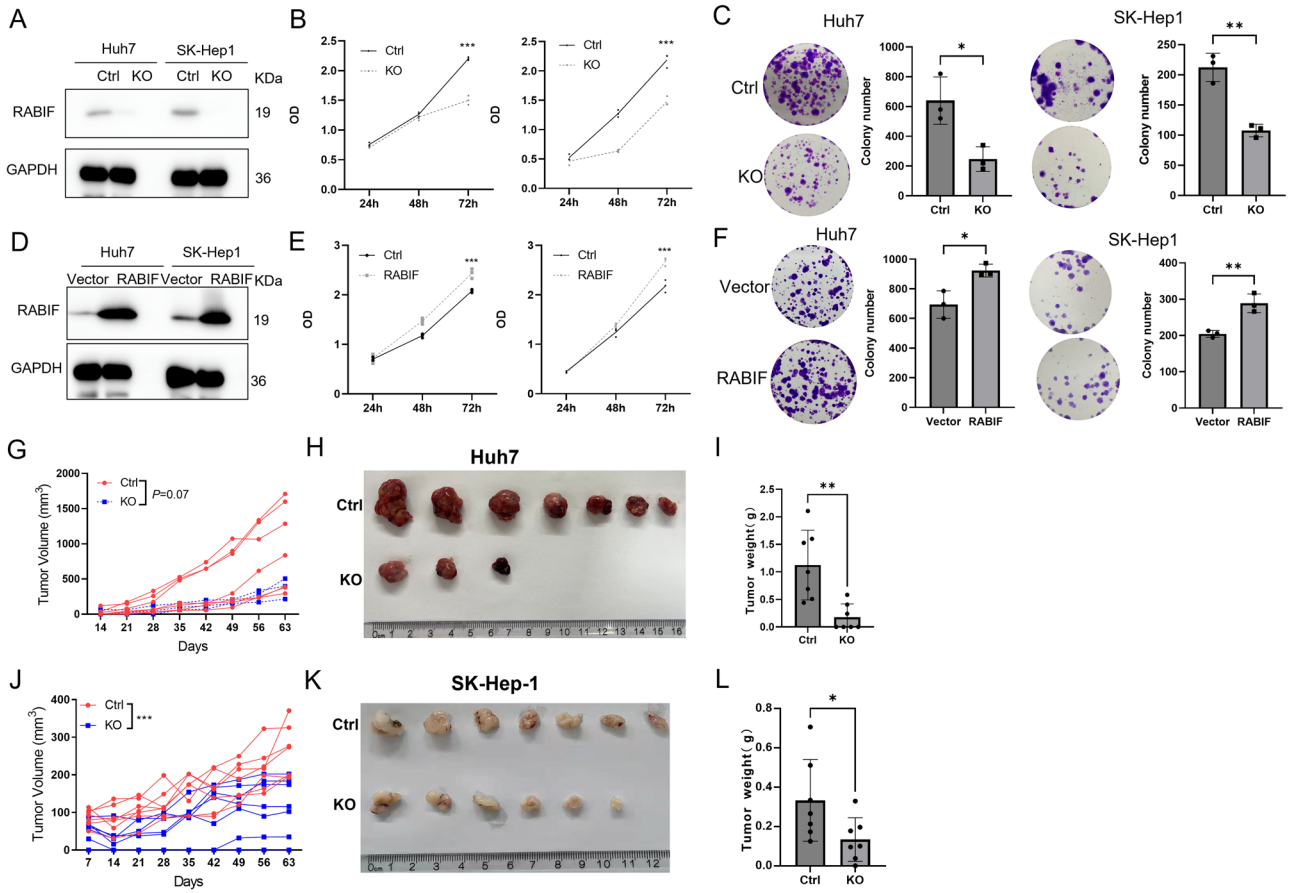

Fig. 2 | RABIF promotes HCC proliferation. A CRISPR/Cas9-mediated knockout of RABIF was confirmed by western blot in Huh7 and SK-Hep1 cells. **B** Cell proliferation was determined by CCK-8 assay. **C** Representative images (left) and quantification of colonies (right) from control and RABIF KO cells ($n = 3$ per cell type). **D** Overexpression of RABIF in Huh7 and SK-Hep1 cells was validated by immunoblot assay. **E** Cell proliferation of control and RABIF overexpression cells was compared by CCK-8 assay. **F** Representative images (left) and quantification of colonies (right) from control and RABIF overexpression cells ($n = 3$ per cell type). **G–L** Tumor growth curve (**G, J**), xenograft tumors (**H, K**) and tumor weight (**I, L**) in the subcutaneous implantation mouse model ($n = 7$ for each group). **B, E, G, J** Two-way ANOVA; (**C, F, I, L**) Unpaired t-test. $^{*}p < 0.05$, $^{**}p < 0.01$, $^{***}p < 0.001$.

conducted real-time quantitative PCR analysis using a tumor cDNA microarray, including 20 paired HCC tissues. The analysis showed that RABIF was upregulated in 15/20 liver tumor samples compared to the matched nonmalignant liver, with 9 of 20 (45%) showing a 1.5-fold or greater increase (Fig. 1H). Next, we explored the clinical relevance of RABIF for HCC. Analysis of HCC patient survival according to RABIF mRNA expression using the KM plotter showed that high expression of RABIF was associated with worse overall and disease-free survival (Fig. 1I and J). Taken together, these data establish that RABIF is highly expressed in HCC and correlates with poor prognosis in patients with liver cancer.

RABIF promotes HCC cell growth in vitro and in vivo

Considering the negative correlation between RABIF expression and HCC patient survival, we examined the functional impact of RABIF in HCC cells. We first established RABIF-depleted Huh7 cells, a commonly used HCC cell line, and SK-Hep1 cells. Although SK-Hep1 has been historically classified as a hepatocellular carcinoma cell line, more recent studies suggest that it may more accurately represent liver sinusoidal endothelial cells[25]. For the purposes of this study, SK-Hep1 cells were used as a liver cell model in the context of RABIF depletion, acknowledging the potential difference in cellular origin. Successful knockout of RABIF expression was validated by western blotting and Sanger sequencing (Fig. 2A, Supplementary Fig. 1). We observed that the proliferation of RABIF-depleted cells was slowed down compared to control cells, although this effect was not evident during the first 24 hours in HuH7 cells or the second 24 hours in SK-Hep1 cells. (Fig. 2B). To further confirm the oncogenic effects of RABIF on HCC cells, we performed a colony formation assay in Huh7 and SK-Hep1 cells that did not express RABIF. As shown in Fig. 2C, RABIF knockout led to a significant decrease in the colony number of HCC cells. Conversely, overexpression of RABIF in Huh7 and SK-Hep1 cells markedly promoted HCC cell growth (Fig. 2D and E). In addition, overexpression of RABIF enhanced the colony formation ability of HCC cells compared to that of control cells (Fig. 2F). Next, we introduced a CRISPR/Cas9–resistant RABIF (with a synonymous mutation that disrupts the protospacer adjacent motif) in RABIF-KO HCC cells (Supplementary Fig. 2A). The expression of the exogenous RABIF successfully restored the impaired growth and colony formation observed in RABIF-KO HCC cells (Supplementary Fig. 2B and C).

Next, we determined the role of RABIF in the development of HCC. Nude mice were inoculated with either control or RABIF depletion HCC cell lines. Although RABIF depletion appears to inhibit Huh7 xenograft tumor growth, a marked reduction in both tumor growth and tumor weight was observed in Sk-Hep1 xenograft models (Fig. 2G–L). Collectively, these results validated the oncogenic function of RABIF in HCC.

RABIF regulates mitophagy through interaction with STOML2

To gain insight into the potential mechanism that mediates the oncogenic function of RABIF in liver cancer cells, we performed immunoprecipitation mass spectrometry (IP/MS) analysis to identify proteins associated with RABIF. The previously known RABIF interacting partner RAB10 as well as several other RAB proteins such as RAB1B and RAB8B were immunoprecipitated by RABIF (Fig. 3A and Supplementary Table 2). Unexpectedly,

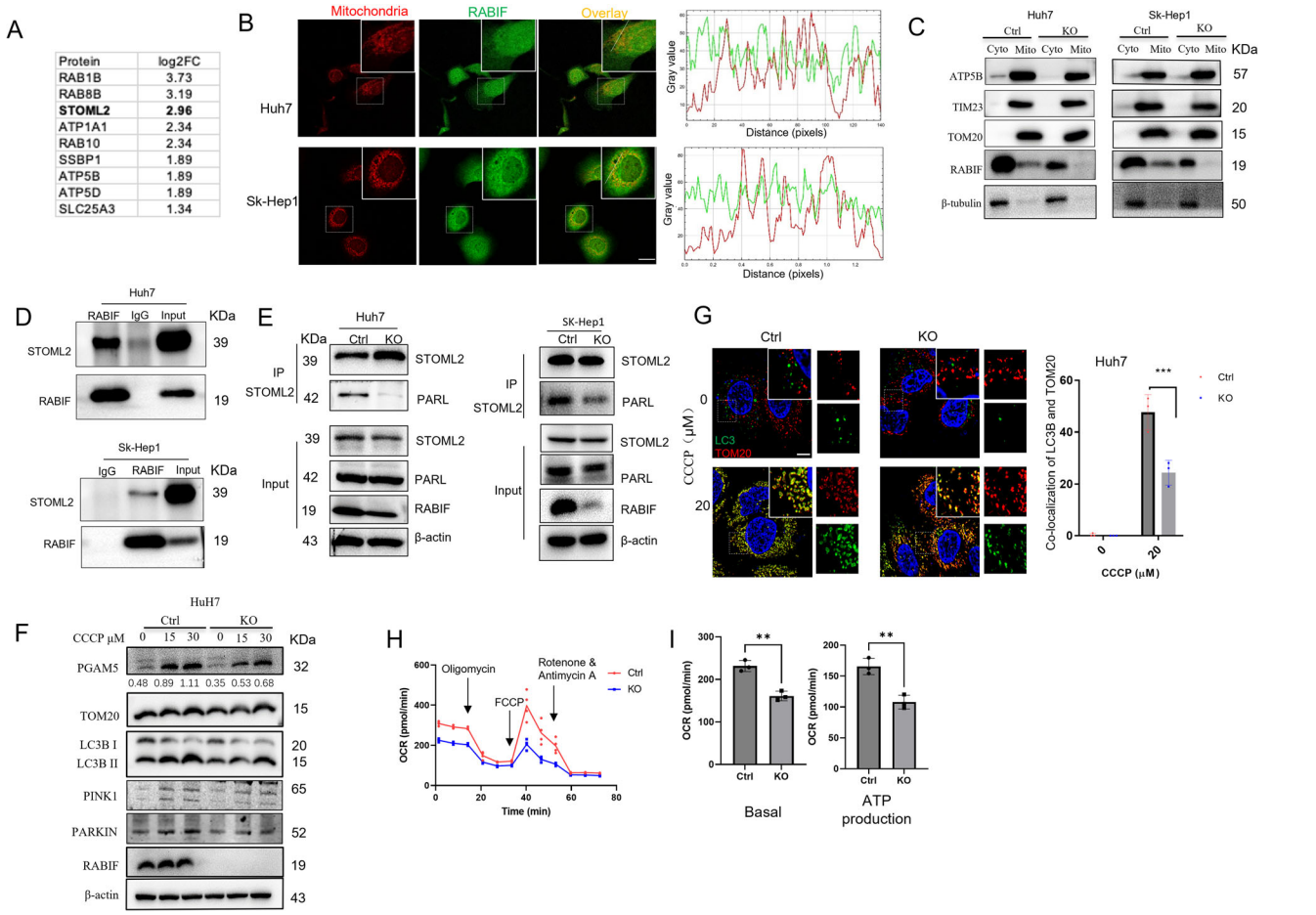

Fig. 3 | RABIF regulates mitophagy in HCC. A RABIF-interacting proteins were identified using immunoprecipitation mass spectrometry. Non-tagged RABIF was expressed in Huh7 cells, and co-purified proteins were identified by MS. Representative top hits are displayed. **B** Immunofluorescence study of RABIF protein subcellular localization (green). Mitotracker marks mitochondria. Scale bars,10 μm. Co-localization index of RABIF and mitochondria was calculated by Image J (right). **C** RABIF and the specified components of mitochondrial complex proteins were detected in the cytosolic and mitochondrial fractions using immunoblotting. **D** Immunoprecipitation assay as applied to confirm the interaction between RABIF and STOML2. **E** Cell lysates from control and RABIF KO cells were immunoprecipitated with anti-STOML2 antibody. Bound proteins and total cell lysates were analyzed by immunoblotting with indicated antibodies. **F** Huh7 cells were treated with CCCP for 4 hours, then cell lysates were analyzed by Western blotting with indicated antibodies. The lower band of PGAM5 is the cleavage form. Relative intensities of cleaved PGAM5 were shown below the band. **G** Huh7 control and RABIF KO cells were treated with CCCP for 4 hours. To assess mitophagy, the cells were fixed and immunostained for LC3 (red) and TOM20 (green). The graph shows the LC3/TOM20 colocalization puncta per cell calculated by ImageJ. Scale bar: 10 μm. **H, I** Seahorse measurements of the oxygen consumption rate (OCR) (**H**) and their corresponding metabolic rates in (**I**) in control and RABIF KO Huh7 cells. **G** Two-way ANOVA. **I** Unpaired t-test. $^{**}p < 0.01$, $^{***}p < 0.001$.

this analysis also identified many previously unknown mitochondrial proteins such as STOML2, ATP5B, and ATP5D, suggesting that RABIF may regulate mitochondrial function in HCC (Fig. 3A). To address the involvement of RABIF in regulating mitochondrial function, we first examined its subcellular localization. Using confocal microscopy, we observed that endogenous RABIF was primarily located in the cytoplasm and, to a lesser extent, in the mitochondria. This was confirmed by co-staining with MitoTracker (Fig. 3B). To confirm the presence of RABIF in mitochondria, we fractionated the cytoplasm and mitochondria and then conducted immunoblotting with antibodies against RABIF and three other mitochondrial proteins, TIM23, TOM20, and ATP5B (Fig. 3C). We detected RABIF not only in the cytoplasm but also in the mitochondria, as confirmed by knockout of RABIF using the Crispr/Cas9 system (Fig. 3C).

We selected STOML2 for further study due to its reported role in the mitophagy process and its essential function in Hepatocellular Carcinoma (HCC)[8,26,27]. The interaction between RABIF and STOML2 was confirmed by immunoprecipitation in Huh7 and Sk-Hep1 cells (Fig. 3D). It has been reported that STOML2 regulates the activity of rhomboid protease presenilin-associated rhomboid-like protein (PARL) via forming a protease complex with it[28]. To test whether RABIF mediates this interaction, we immunoprecipitated STOML2 in control and RABIF KO cells and detected PARL by immunoblotting. Intriguingly, our results showed that the knockout of RABIF markedly mitigated the physical interaction between endogenous STOML2 and PARL (Fig. 3E).

The mitochondrial Ser/Thr protein phosphatase phosphoglycerate mutase 5 (PGAM5) is a substrate of PARL[29]. Processed PGAM5 by PARL has been proposed to be involved in the regulation of mitophagy[30]. Therefore, we next attempted to determine whether knockout of RABIF impairs mitophagy in HCC cells through the PARL-PGAM5 axis. Indeed, we observed less cleaved PGAM5 in RABIF-deficient cells than in wild-type cells treated with CCCP (Fig. 3F, Supplementary Fig. 3A). Expression of the CCCP-induced autophagy marker LC3B II was also decreased when RABIF was knocked out (Fig. 3F, Supplementary Fig. 3A). In addition, colocalization of endogenous LC3 with TOM20 was markedly decreased in RABIF KO cells treated with CCCP (Fig. 3G, Supplementary Fig. 3B). These results indicate that depletion of RABIF inhibits mitophagy in HCC.

Mitophagy is a type of selective autophagy that modulates mitochondrial content to maintain energy metabolism[31]. It has been reported that

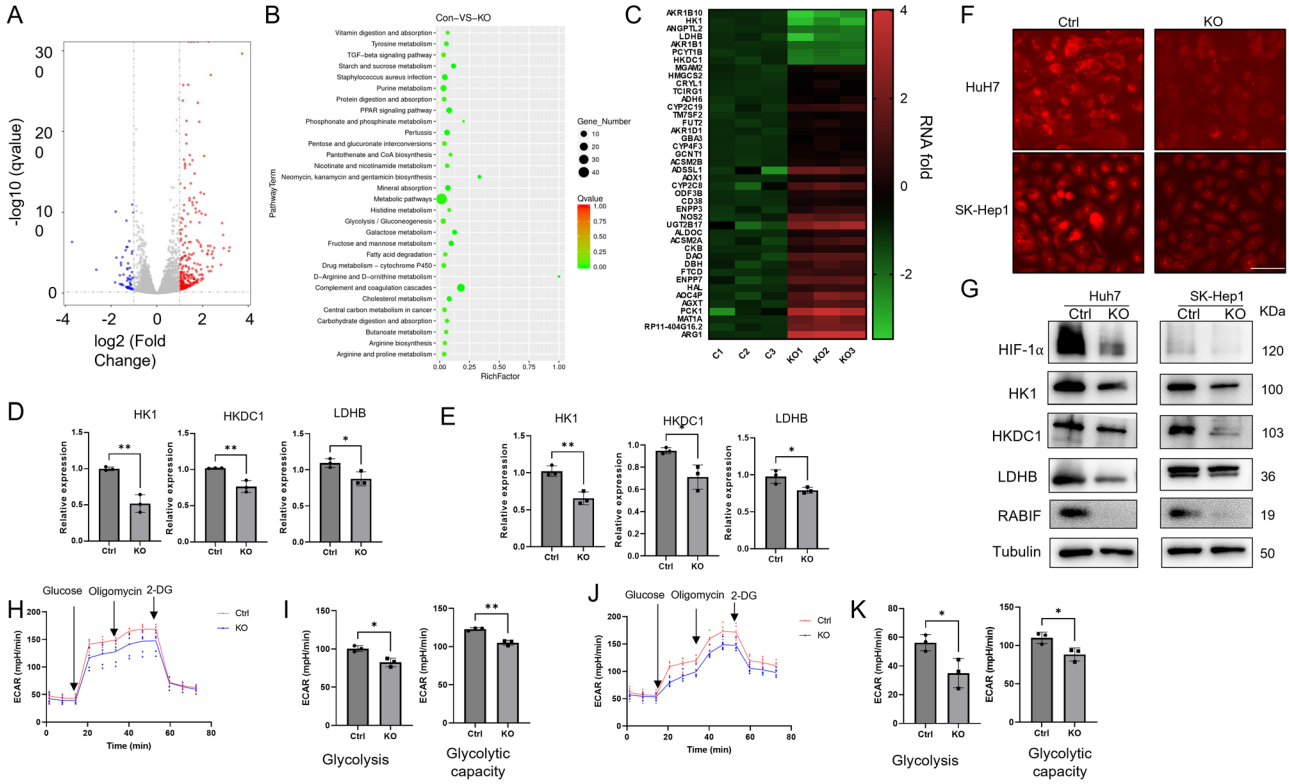

Fig. 4 | RABIF regulates glycolysis in HCC. (**A**) The volcano plot of statistical significance ($p < 0.05$) versus fold change (ratio of KO/Ctr group) shows the most substantially differentially expressed genes by genome-wide transcriptome analysis between Ctr and RABIF KO Huh7 cells ($n = 3$). **B** KEGG pathway enrichment analysis of the entire list of differentially expressed genes. **C** Color-coded heat map of differentially expressed genes from the glucose metabolism pathway. **D, E** qRT-PCR assay to validate the expression change of glycolytic genes in Huh7 (**D**) and SK-Hep1 (**E**) cells. **F** Microscopic analysis of mitoROS production in HCC cells with or without RABIF knockout. HCC cells were stained with 1 μM MitoSOX, fixed and subjected to imaging. Scale bar: 50μm. **G** HIF1α and glycolytic enzymes were determined by western blotting in control or RABIF depletion HCC cells treated with $CoCl_2$ for 48 h. (**H-K**) Extracellular acidification rate (ECAR) (H, **J**) and their corresponding metabolic rates (**I, K**) were measured by seahorse in Huh7 (**H, I**) and SK-Hep1 cells (**J, K**). **D, E, I, K** Unpaired t-test. *p < 0.05, **$p < 0.01$, ***$p < 0.001$, ****$p < 0.0001$.

mitophagy is involved in HCC progression by regulating metabolism reprogramming[32]. To explore whether RABIF regulates HCC metabolism, we conducted seahorse analysis to measure the oxygen consumption (OCR) in HCC cells. The results showed that depletion of RABIF led to a decrease in OCR, including basal respiration and ATP production (Figs. 3H, I, Supplementary Fig. 3C, D), revealing that knockout of RABIF also impaired mitochondrial metabolism.

RABIF regulates glycolysis in liver cancer cells

The metabolic shift from mitochondrial to glycolytic metabolism for adapting to the surrounding environment is a distinctive feature of most cancer cells, including HCC[33,34]. To study whether depletion of RABIF is involved in a metabolic shift in HCC cells, we performed genome-wide transcriptomic analysis by RNA sequencing in RABIF-knockout Huh7 cells. We identified 342 differentially expressed genes between RABIF knockout cells and control cells, comprising 287 upregulated and 55 downregulated genes (Fig. 4A). KEGG pathway analyses revealed that the metabolic pathway was the most affected pathway upon RABIF knockout (Fig. 4B), consisting of 42 differentially expressed genes (Fig. 4C). Among these, we found three of the most downregulated genes, HK1, LDHB, and HKDC1, were involved in glycolysis (Fig. 4C). As dysregulation of glycolysis has been shown to play an important role in HCC, we therefore examined the expression of HK1, LDHB and HKDC1 in control and RABIF KO cells by qPCR. The results clearly showed that RABIF depletion significantly reduced HK1, LDHB and HKDC1 expression (Fig. 4D, E).

HIF-1α is a shared element in pathways responsible for regulating cellular metabolism. Many glycolytic genes have been identified as targets of HIF-1α in HCC[33,35]. It has been reported that mitoROS are responsible for the stabilization of HIF-1α[36,37]. As mitophagy is a widely acknowledged process to remove compromised mitochondria that generate elevated levels of mitoROS[38], we therefore hypothesized that RABIF regulated glycolytic gene expression through mitoROS-mediated HIF-1α activation. To validate this hypothesis, we used MitoSOX to measure mitoROS production in HCC cells. We found that depleting RABIF significantly decreased mitoROS production (Fig. 4F). In line with this discovery, we noted a decrease in the protein expression of HIF-1α and its glycolytic target genes, including HK1, LDHB, and HKDC1 (Fig. 4G).

To further test whether RABIF regulates glycolytic flux, we investigated the effect of RABIF depletion on glycolysis by measuring the extracellular acidification rate (ECAR). We observed a marked decrease in the basal glycolysis and glycolytic capacity in RABIF knockout cells compared to control cells (Fig. 4H-K), suggesting that RABIF is essential for glycolysis in liver cancer cell. Taken together, these data indicated that RABIF depletion affects glycolysis in HCC cells.

RABIF enhances RAB10-mediated glucose uptake in HCC

RABIF has been reported to act as a RAB-stabilizing chaperone of RAB10 to mediate glucose uptake in adipocytes[19]. To test whether RABIF was involved in glucose uptake in HCC cells, we first validated the interaction between RABIF and RAB10 in HCC cells. Immunoprecipitation experiments confirmed their interaction in Huh7 and SK-Hep1 cells (Fig. 5A). We also found that RABIF depletion led to a significant decrease in RAB10 expression (Fig. 5B). The knockout of RABIF markedly inhibited glucose uptake, whereas overexpression of RAB10 in RABIF depletion cells could partially rescue glucose uptake (Fig. 5C, D). Moreover, enforced expression of RAB10 could also restore the cell growth and colony formation defects mediated by

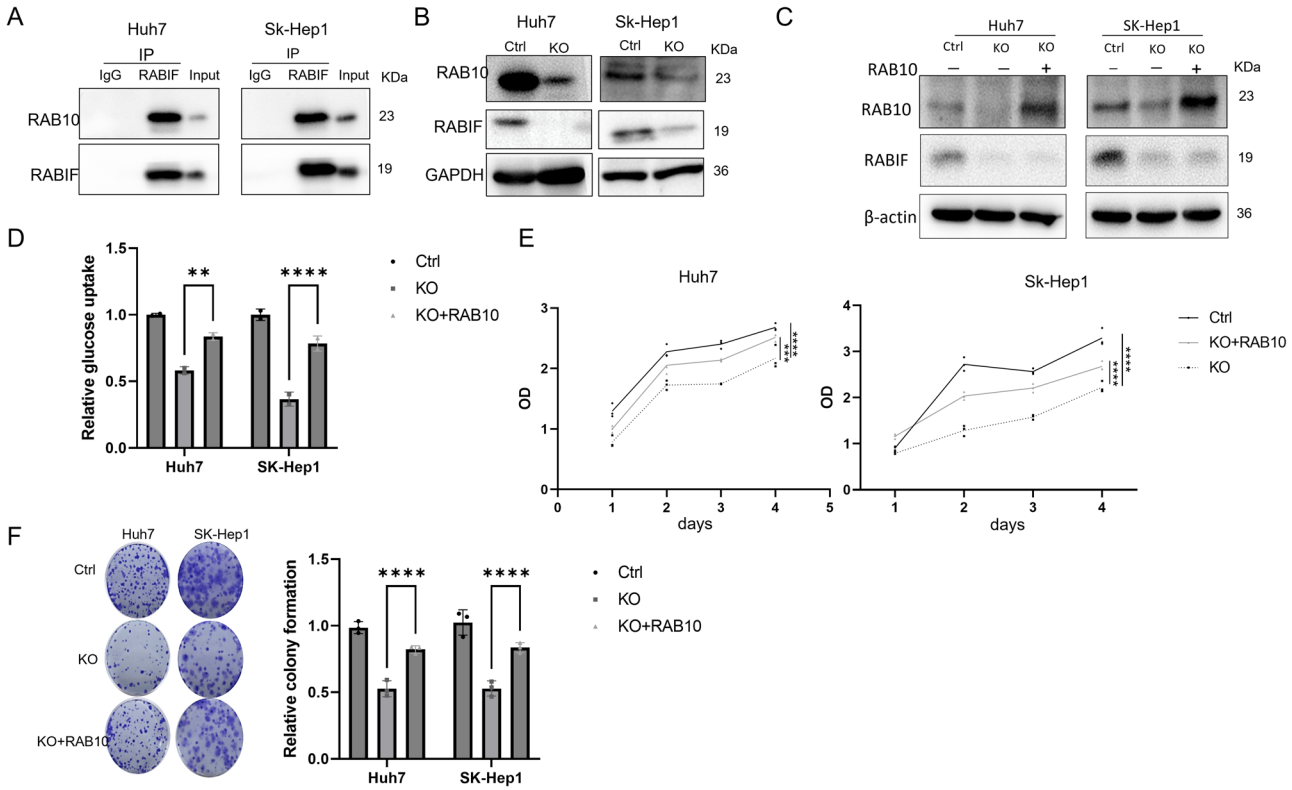

Fig. 5 | RABIF regulates glucose uptake via RAB10. A The interaction between RABIF and RAB10 was confirmed by immunoprecipitation assay. **B** RAB10 expression was detected in control and RABIF KO cells by western blotting. **C** Rescue expression of RAB10 in RABIF KO cells was validated by western blot. **D** Glucose uptake was measured in control and RABIF KO cells. **E, F** Overexpression of RAB10 restored cell proliferation (**E**) and colony formation (**F**) of RABIF KO cell. **D, E, F** Two-way ANOVA. $^{*}p < 0.05$, $^{**}p < 0.01$, $^{***}p < 0.001$.

RABIF depletion (Fig. 5E, F). Collectively, our results highlight the important role of the RABIF-RAB10 axis in mediating glucose metabolism and tumor cell growth in HCC.

RABIF confers sorafenib resistance to HCC by regulating mitophagy

Previous studies have demonstrated that mitophagy promotes resistance to sorafenib in HCC[39,40]. Considering the role of RABIF in mitophagy, we investigated whether RABIF was involved in sorafenib resistance. We first analyzed the correlation between RABIF expression and the prognosis of sorafenib-treated HCC patients. The results showed that high expression of RABIF was correlated with worse patient survival (Supplementary Fig. 4A). To further confirm the role of RABIF in sorafenib resistance, we compared the IC50 between wild-type cells and RABIF-knockout cells. We found that RABIF depletion significantly decreased the IC50 in HCC cells (Fig. 6A, B). In addition, sorafenib treatment induced much more apoptosis in RABIF-knockout cells than in control cells (Fig. 6C-F). Noteworthy, knockout RABIF induced a slighter more apoptosis of HCC cells without sorafenib treatment, suggesting that the comprised mitochondria may be undergo apoptosis when loss of RABIF blocking mitophagy. Moreover, we used xenograft tumor models to evaluate whether the knockout of RABIF could enhance sorafenib-induced tumor inhibition in vivo. Consistent with the in vitro data, the depletion of RABIF markedly promoted the tumor-inhibitory effects of sorafenib (Fig. 6G-J). To determine whether knockout of RABIF sensitizes HCC cells to sorafenib by regulating mitophagy, we treated HCC cells with sorafenib and examined mitophagy by western blotting. Our results indicated that sorafenib treatment induced more PGAM5 cleavage and LC3B II in control cells than in RABIF KO cells (Fig. 6K). The immunofluorescence assay also showed that knockout of RABIF significantly reduced sorafenib-induced co-localization of LC3B and Tom20 (Fig. 6L, M). To further confirm that RABIF-mediated mitophagy is involved in the anticancer effects of sorafenib, we treated HCC cells with Mdivi-1, a mitophagy inhibitor, and found that Mdivi-1 treatment inhibited HCC cell proliferation in a dose-dependent manner (Supplementary Fig. 4B). Co-treatment of HCC cells with Mdivi-1 and sorafenib synergistically inhibits HCC growth. More importantly, RABIF knockout further enhanced the synergistic effects of Mdivi-1 and sorafenib (Supplementary Fig. 4C). Taken together, these data suggest that RABIF-mediated mitophagy is involved in sorafenib resistance in HCC cells.

Discussion

In this study, we provide novel evidence for an essential role of RABIF in HCC. Our data reveal that RABIF is upregulated in HCC and promotes HCC cell growth. We found that RABIF was mainly distributed in the cytoplasm and partly in the mitochondria. Cytosolic RABIF regulates glucose uptake in a RAB10-dependent manner. Upon localization to the mitochondria, RABIF exhibited a discernible interaction with STOML2. The ablation of RABIF led to a consequential reduction in PARL activity, primarily attributed to the diminished interaction between STOML2 and PARL. Consequently, the processing of PGAM5 and the subsequent mitophagy orchestrated by PGAM5 were impeded following RABIF knockout. This disruption in cellular processes resulted in the suppression of mitoROS production and downregulation of HIF1α expression. Ultimately, these molecular perturbations culminated in a discernible reduction in the expression of glycolytic genes.

Accumulating evidence indicates that RABIF possesses oncogenic potential in cancers, including HCC[41–43]. However, the underlying mechanism of RABIF in HCC is unexplored. Our IP/MS analysis shows that RABIF associates with multiple mitochondrial proteins, suggesting it may be involved in mitochondrial regulation. Indeed, we confirmed its mitochondrial localization through immunofluorescence and subcellular

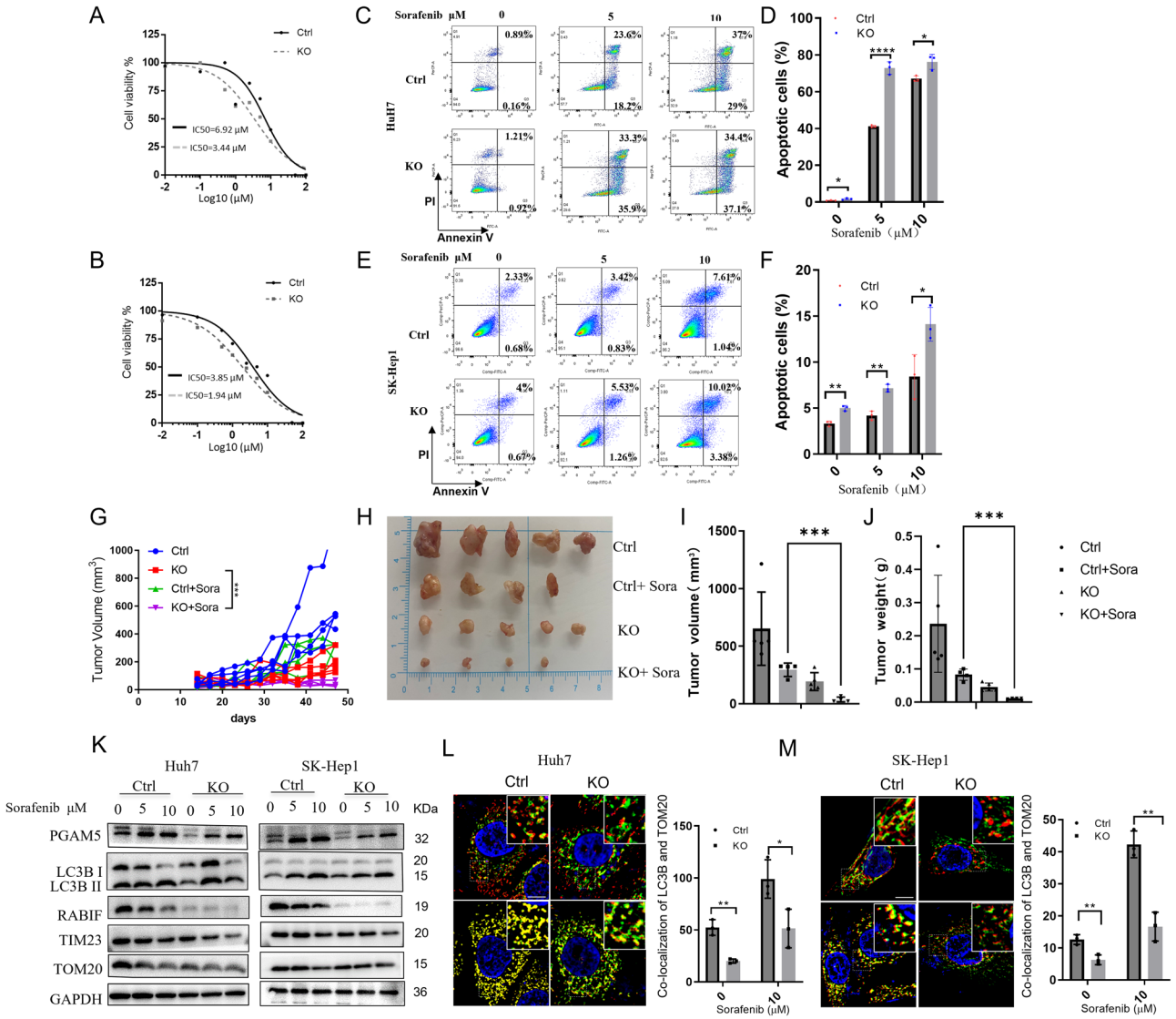

Fig. 6 | RABIF confers sorafenib resistance in HCC. A, B The half inhibitory concentration (IC50) of sorafenib in the respective groups was determined. **C–F** Flowcytometry analysis of sorafenib-induced apoptosis in control and RABIF KO Huh7 (**C, D**) and SK-Hep1 (**E, F**) cells. The cells were treated with sorafenib as indicated dose for 72 h. The graph shows the percentage of apoptotic cells. **G-J** Tumor growth curve (**G**), representative xenograft tumors (**H**), tumor volumes and tumor weight (**J**) in the indicated groups ($n = 5$). Sorafenib was intraperitoneally injected at 30 mg/kg for two weeks. **K** Immunoblot showing expression levels of indicated proteins in control or RABIF KO cells treated with sorafenib for 48 h. **L** Control and KO cells were treated with sorafenib for 12 h. Then the cells were fixed and stained with LC3 (red) and TOM20 (green). The graph shows the LC3/TOM20 colocalization puncta per cell calculated by ImageJ (right). **M** Similar analysis as in **K** was performed in SK-Hep1 cells. **D, F, G, M** Two-way ANOVA; (**I, J**) One-way ANOVA. $^{*}p < 0.05$, $^{**}p < 0.01$, $^{***}p < 0.001$, $^{****}p < 0.0001$.

fractionation assays. The interaction between RABIF and STOML2 was further validated.

STOML2 is a mitochondrial protein and acts as a scaffold to promote STOML2-PARL-YME1L complex formation. The formation of this complex influences PARL-mediated processing of both PINK1 and PGAM5[28]. Our results indicate that the knockout of RABIF disrupts the interaction between STOML2 and PARL and impairs PGAM5 processing. Recent research has underscored the significance of PGAM5 in various cellular processes associated with cancer, including mitophagy[44]. Dephosphorylation of FUNDC1 and stabilization of PINK1 have been found crucial for PGAM5-mediated mitophagy[45,46]. Further study is needed to identify the downstream effectors involved in the RABIF-STOML2-PGAM5 axis-mediated mitophagy in HCC.

Recently, many studies have demonstrated that RAB GTPases function as important regulators of hepatocellular metabolism. For example, RAB32 binds to lysosomes and regulates Hep3B proliferation and cell growth by controlling lysosomal mTOR trafficking[47]. RAB24 is increased in individuals with non-alcoholic fatty liver disease (NAFLD) and regulates blood glucose homeostasis by increasing mitochondrial plasticity[48]. As an RAB-interacting factor, whether RABIF was involved in RAB-mediated hepatocellular metabolism is largely unknown. Our IP-MS study revealed that RABIF can interact with several RAB proteins, including RAB10. We further validated that RABIF regulates glucose uptake in a RAB10-dependent manner. Additionally, we demonstrated that depletion of RABIF inhibited glycolysis by reducing glycolytic gene expression. Mechanistic studies indicated that RABIF deficiency led to a decrease of mitoROS production and subsequent destabilization of HIF1α, which is critical for activating glycolytic gene expression[49,50]. These findings uncover a novel role of RABIF in glucose metabolism in HCC.

It has been shown that RAB10 is involved in hepatocellular metabolism by regulating low-density lipoproteins (LDLs) uptake and lipophagy[51–53]. Indeed, in our RNA-seq analysis, we found that RABIF knockout also affected fatty acid and cholesterol metabolism. This finding implies that RABIF may potentially engage in lipid metabolism in

hepatocytes and that RABIF may also promotes HCC progression through this mechanism.

Since it was the first treatment to be approved for HCC, sorafenib is still one of the most common first-line therapies for this condition. However, the impact of sorafenib on tumor response in pivotal clinical trials was attenuated, attributed to the presence of cell resistance to sorafenib[54,55]. Recent studies indicated that mitophagy was involved in sorafenib resistance in HCC[39,56,57]. Consistent with these findings, our results indicated that RABIF confers resistance to sorafenib in HCC. Suppression of RABIF expression sensitizes HCC cells and xenograft tumors to sorafenib. The combination of the mitophagy inhibitor Mdivi-1 and sorafenib has a synergistic effect on growth arrest in HCC.

In conclusion, our study reveals that elevated RABIF plays an essential role in HCC progression and sorafenib resistance. Our findings suggest that targeting RABIF may provide novel therapeutic strategy for HCC.

Methods

Cell culture

Huh7 and Sk-Hep1 human liver cancer cell lines were obtained from Shanghai Cell Line Bank of the Chinese Academy of Sciences (Shanghai, China). All cells were cultured in DMEM supplemented with 10% fetal bovine serum and 1% streptomycin/penicillin, as previously described[58]. To knock out RABIF in HCC cells, a high-scoring guide RNA (target sequence:5′- AGCGAGTTAGTGTCAGCCGA-3′) was designed by CHO PCHOP[59] and cloned into the lentiCRISPRv2 vector. The CRISPR plasmids were transiently transfected into HCC cells for 48 h, after which the cells were passaged and selected using puromycin for 1 week. After which, HCC cells were harvested to determine the KO by using sanger sequence. To prevent the impact of single-clone selection, polyclonal RABIF KO cells were employed.

Cell viability and colony formation analysis

The cells were seeded into 96-well plates at a density of 2×10^3 cells/well. The CCK-8 solution was added to each 96-well at the indicated time points and incubated for 2 h. The absorbance was measured using a microplate reader at 450 nm. To determine the IC50 in HCC cell lines, HCC cells were seeded into 96-well plates and incubated overnight, after which the cells were treated with serial concentrations of sorafenib for 72 h. Cell viability was measured using the CCK-8 assay.

Cells were sown and cultivated for 14 days in the medium for the colony formation experiment. Colonies were stained with 0.5% crystal violet after treatment with a 4% paraformaldehyde solution. ImageJ software was used to count the colonies.

RT-qPCR

TRIZOL (Invitrogen) was used to extract total RNA from HCC cells. The PrimeScript RT Reagent Kit (TAKARA) was used to synthesize cDNA. qPCR tests with SYBR Green probes (Takara) were performed on an Applied Biosystems 7500 Fast Real-Time PCR apparatus. Primer sequences used are listed in Supplementary Table S1.

RNA sequencing

For RNA sequencing, an Agilent 2100 Bioanalyzer (Agilent Technologies, Palo Alto, CA, USA), NanoDrop (Thermo Fisher Scientific Inc.), and 1% agarose gel were used to measure and quantify the total RNA in each sample. A total of 1 μg of RNA with a RIN value of at least 6.5 was utilized to prepare the following library. Next-generation sequencing libraries were prepared following the manufacturer's instructions. Then, in accordance with the manufacturer's recommendations, libraries with various indices were multiplexed and placed on an Illumina HiSeq instrument (Illumina, San Diego, CA, USA). A 2 × 150 bp paired-end (PE) configuration was used for sequencing, and HiSeq Control Software (HCS) + OLB + GAPipeline-1.6 (Illumina) was used for image processing and base calling. The sequences were processed and analyzed using GENEWIZ.

Glucose uptake

The absorption of glucose in Sk-Hep1 or Huh-7 cells (2×10^4) was quantified using the Glucose Uptake Assay kit (#ab136955, Abcam, UK), as per the guidelines provided by the manufacturer. Briefly, cells were incubated with the glucose analog 2-deoxyglucose. The oxidation of the accumulated 2-DG6P produced NADPH, which in turn oxidized a substrate.

Western blotting

Cells were lysed with RIPA buffer containing a protease inhibitor cocktail. A mitochondrial protein extraction kit (KGB5401, KeyGEN, China) was used to extract and isolate mitochondrial and cytoplasmic fractions. The proteins were separated on a 4–12% SDS-PAGE gel, transferred to a PVDF membrane (Bio-Rad), and detected with appropriate antibodies. The RABIF (sc-390759) and PGAM5 (sc-515880) antibodies were obtained from Santa Cruz. The β-actin (AC026), GAPDH (AC002) and β-tubulin (AC008) antibodies were purchased from Abclonal. RAB10 (11808-1-AP), TIM23 (67535-1-Ig), TOM20 (11802-1-AP), ATP5B (17247-1-AP), LC3B (14600-1-AP), STOML2 (60052-1-Ig) antibodies were obtained from Proteintech Group.

Immunofluorescence

The cells were plated on glass slides overnight and then treated progressively in accordance with the applicable experimental conditions for the immunofluorescence test. The cells were then fixed with 3.7% paraformaldehyde and permeabilized with a permeabilizing solution (0.2% [w/v] Triton X-100 in Phosphate buffered saline [PBS]). After blocking with 5% bovine serum albumin C for 30 min at room temperature, the cells were treated with specific antibodies and fluorescence was measured using confocal microscopy (Zeiss).

Immunoprecipitation assay

The cells were lysed with NP40 buffer (50 mmol/L Tris-HCl, pH7.5, 150 mmol/L NaCl, 0.5% NP-40, and 50 mmol/L NaF) containing a cocktail of protease inhibitors. Lysates were treated with primary antibody for 12 h at 4 °C before incubation with protein A/G-Sepharose beads (sc-2003, Santa Cruz) for 4 h at 4 °C. The beads were extracted by centrifugation. After three washes with NP40 buffer, the beads were boiled in 40 μL of loading buffer and analyzed by western blotting.

Seahorse assays

Seahorse assays were performed as previously described[48]. A Seahorse XF 24 Analyzer was used to measure mitochondrial respiration and glycolysis (Agilent Technologies). As a result, 30,000 cells per well were plated on Seahorse cell plates as a monolayer culture. Mitochondrial respiration was achieved by injecting 2 μM oligomycin (Sigma-Aldrich), 1 μM FCCP (Sigma-Aldrich), and 1 μM antimycin A (Sigma-Aldrich) + 1 μM rotenone into the cells (Sigma-Aldrich). Glycolysis was monitored by injecting 100 mM of 2-deoxy-d-glucose (Sigma-Aldrich). The basal OCR and ECAR values indicated the differences observed before and after the addition of oligomycin or glucose. ATP production was calculated by subtracting the OCR after oligomycin injection from the basal respiration level. The glycolysis capacity was determined by subtracting the ECAR before glucose addition from the ECAR after oligomycin treatment.

Xenograft tumor assays

The Xuzhou Medical University Animal Care Committee approved the use of animals in this study. Male nude mice ($n = 7$) were subcutaneously injected with 1×10^6 hepatocellular carcinoma (HCC) cells. The tumor size was measured at the indicated time points using calipers. For sorafenib treatment assays, when tumor growth reached approximately 100 mm^3, the mice were randomly divided into four groups ($n = 5$) and administered either vehicle or sorafenib. The mice were euthanized by CO_2 after 21 days of therapy, and the tumors were collected and weighed.

Statistics and reproducibility

All results are reported as the mean ± SD of at least three replicate studies. GraphPad Prism version 9.3.0 was used for statistical analysis. Student's t-test and one- or two-way ANOVA were used for comparisons between groups. $^{*}P < 0.05$; $^{**}P < 0.01$; $^{***}P < 0.001$; $^{****}P < 0.0001$.

Reporting summary

Further information on research design is available in the Nature Portfolio Reporting Summary linked to this article.

Data availability

RNA sequencing data have been deposited in GEO under study accession no. GSE278116. The source data for graphs are available in Supplementary Data 1. Upon request, the corresponding author will provide access to all the data collected for the study.

Code availability

Not applicable.

Received: 8 January 2024; Accepted: 7 October 2024;
Published online: 16 October 2024

References

1. Bray, F. et al. GLOBOCAN estimates of incidence and mortality worldwide for 36 cancers in 185 countries. *CA Cancer J. Clin.* **68**, 394–424 (2018).
2. Yarchoan, M. et al. Recent Developments and Therapeutic Strategies against Hepatocellular Carcinoma. *Cancer Res* **79**, 4326–4330 (2019).
3. Beyoglu, D. et al. Tissue metabolomics of hepatocellular carcinoma: tumor energy metabolism and the role of transcriptomic classification. *Hepatology* **58**, 229–238 (2013).
4. Lee, Y.-K. et al. Lactate-mediated mitoribosomal defects impair mitochondrial oxidative phosphorylation and promote hepatoma cell invasiveness. *J. Biol. Chem.* **292**, 20208–20217 (2017).
5. Jin, T. et al. Mitochondrial metabolic reprogramming: An important player in liver cancer progression. *Cancer Lett.* **470**, 197–203 (2020).
6. Panigrahi, D. P. et al. The emerging, multifaceted role of mitophagy in cancer and cancer therapeutics, *Semin. Cancer Biol.* Elsevier, 2020, pp. 45–58.
7. Macleod, K. F. Mitophagy and mitochondrial dysfunction in cancer. *Annu. Rev. Cancer Biol.* **4**, 41–60 (2020).
8. Zheng, Y. et al. STOML2 potentiates metastasis of hepatocellular carcinoma by promoting PINK1-mediated mitophagy and regulates sensitivity to lenvatinib. *J. Hematol. Oncol.* **14**, 1–18 (2021).
9. Zhou, J. et al. Simultaneous treatment with sorafenib and glucose restriction inhibits hepatocellular carcinoma in vitro and in vivo by impairing SIAH1-mediated mitophagy. *Exp. Mol. Med.* **54**, 2007–2021 (2022).
10. Rojas, A. M., Fuentes, G., Rausell, A. & Valencia, A. The Ras protein superfamily: evolutionary tree and role of conserved amino acids. *J. Cell Biol.* **196**, 189–201 (2012).
11. Stenmark, H. Rab GTPases as coordinators of vesicle traffic. *Nat. Rev. Mol. Cell Biol.* **10**, 513–525 (2009).
12. Goldenring, J. R. A central role for vesicle trafficking in epithelial neoplasia: intracellular highways to carcinogenesis. *Nat. Rev. Cancer* **13**, 813–820 (2013).
13. Mizuno-Yamasaki, E., Rivera-Molina, F. & Novick, P. GTPase networks in membrane traffic. *Annu Rev. Biochem* **81**, 637–659 (2012).
14. Shafique, A., Brughera, M., Lualdi, M. & Alberio, T. The Role of Rab Proteins in Mitophagy: Insights into Neurodegenerative Diseases. *Int. J. Mol. Sci.* **24**, 6268 (2023).
15. Heo, J.-M. et al. RAB7A phosphorylation by TBK1 promotes mitophagy via the PINK-PARKIN pathway. *Sci. Adv.* **4**, eaav0443 (2018).
16. Lai, Y. C. et al. Phosphoproteomic screening identifies Rab GTP ases as novel downstream targets of PINK 1. *EMBO J.* **34**, 2840–2861 (2015).
17. Moya, M., Roberts, D. & Novick, P. DSS4-1 is a dominant suppressor of sec4-8 that encodes a nucleotide exchange protein that aids Sec4p function. *Nature* **361**, 460–463 (1993).
18. Wixler, V. et al. Identification and characterisation of novel Mss4-binding Rab GTPases. *Biol. Chem.* **392**, 239–248 (2011).
19. Gulbranson, D. R. et al. RABIF/MSS4 is a Rab-stabilizing holdase chaperone required for GLUT4 exocytosis. *Proc. Natl Acad. Sci. USA* **114**, E8224–E8233 (2017).
20. Jeng, E. E. et al. Systematic Identification of Host Cell Regulators of Legionella pneumophila Pathogenesis Using a Genome-wide CRISPR Screen. *Cell Host Microbe* **26**, 551–563 e556 (2019).
21. Liu, C. et al. Bromo-and extraterminal domain protein inhibition improves immunotherapy efficacy in hepatocellular carcinoma,. *Cancer Sci.* **111**, 3503–3515 (2020).
22. Wang, W., Jia, W. D., Hu, B. & Pan, Y. Y. RAB10 overexpression promotes tumor growth and indicates poor prognosis of hepatocellular carcinoma. *Oncotarget* **8**, 26434–26447 (2017).
23. Kudo, M. et al. Sorafenib plus low-dose cisplatin and fluorouracil hepatic arterial infusion chemotherapy versus sorafenib alone in patients with advanced hepatocellular carcinoma (SILIUS): a randomised, open label, phase 3 trial. *Lancet Gastroenterol. Hepatol.* **3**, 424–432 (2018).
24. Tang, W. et al. The mechanisms of sorafenib resistance in hepatocellular carcinoma: theoretical basis and therapeutic aspects. *Signal Transduct. Target. Ther.* **5**, 87 (2020).
25. Tai, Y. et al. SK-Hep1: not hepatocellular carcinoma cells but a cell model for liver sinusoidal endothelial cells. *Int. J. Clin. Exp. Pathol.* **11**, 2931 (2018).
26. Liu, Y. et al. Targeting SLP2-mediated lipid metabolism reprograming restricts proliferation and metastasis of hepatocellular carcinoma and promotes sensitivity to Lenvatinib. *Oncogene* **42**, 374–388 (2023).
27. Qin, C. et al. STOML2 restricts mitophagy and increases chemosensitivity in pancreatic cancer through stabilizing PARL-induced PINK1 degradation. *Cell Death Dis.* **14**, 191 (2023).
28. Wai, T. et al. The membrane scaffold SLP2 anchors a proteolytic hub in mitochondria containing PARL and the i-AAA protease YME1L,. *EMBO Rep.* **17**, 1844–1856 (2016).
29. Sekine, S. et al. Rhomboid protease PARL mediates the mitochondrial membrane potential loss-induced cleavage of PGAM5. *J. Biol. Chem.* **287**, 34635–34645 (2012).
30. Yan, C. et al. PHB2 (prohibitin 2) promotes PINK1-PRKN/Parkin-dependent mitophagy by the PARL-PGAM5-PINK1 axis. *Autophagy* **16**, 419–434 (2020).
31. Palikaras, K., Lionaki, E. & Tavernarakis, N. Balancing mitochondrial biogenesis and mitophagy to maintain energy metabolism homeostasis. *Cell Death Differ.* **22**, 1399–1401 (2015).
32. Zhao, Y. et al. Nuclear-encoded lncRNA MALAT1 epigenetically controls metabolic reprogramming in HCC cells through the mitophagy pathway. *Mol. Ther.-Nucleic Acids* **23**, 264–276 (2021).
33. Sakamoto, A. et al. Lysine demethylase LSD1 coordinates glycolytic and mitochondrial metabolism in hepatocellular carcinoma cells. *Cancer Res.* **75**, 1445–1456 (2015).
34. Zhang, Z. et al. MFN1-dependent alteration of mitochondrial dynamics drives hepatocellular carcinoma metastasis by glucose metabolic reprogramming. *Br. J. cancer* **122**, 209–220 (2020).
35. Yao, L. et al. Reciprocal REGγ-mTORC1 regulation promotes glycolytic metabolism in hepatocellular carcinoma,. *Oncogene* **40**, 677–692 (2021).
36. Marinaccio, C. et al. LKB1/STK11 is a tumor suppressor in the progression of myeloproliferative neoplasms. *Cancer Discov.* **11**, 1398–1410 (2021).

37. Heher, P. et al. Interplay between mitochondrial reactive oxygen species, oxidative stress and hypoxic adaptation in facioscapulohumeral muscular dystrophy: Metabolic stress as potential therapeutic target. *Redox Biol.* **51**, 102251 (2022).
38. Schofield, J. H. & Schafer, Z. T. Mitochondrial reactive oxygen species and mitophagy: a complex and nuanced relationship. *Antioxid. redox Signal.* **34**, 517–530 (2021).
39. Wu, H. et al. Mitophagy promotes sorafenib resistance through hypoxia-inducible ATAD3A dependent Axis. *J. Exp. Clin. Cancer Res.* **39**, 1–16 (2020).
40. Yao, J. et al. CDK9 inhibition blocks the initiation of PINK1-PRKN-mediated mitophagy by regulating the SIRT1-FOXO3-BNIP3 axis and enhances the therapeutic effects involving mitochondrial dysfunction in hepatocellular carcinoma, *Autophagy*, 1–19 (2021).
41. Huang, W.-C. et al. Identification of the novel tumor suppressor role of FOCAD/miR-491-5p to inhibit cancer stemness, drug resistance and metastasis via regulating RABIF/MMP signaling in triple negative breast cancer. *Cells* **10**, 2524 (2021).
42. Świtnicki, M. P., Juul, M., Madsen, T., Sørensen, K. D. & Pedersen, J. S. PINCAGE: probabilistic integration of cancer genomics data for perturbed gene identification and sample classification. *Bioinformatics* **32**, 1353–1365 (2016).
43. Chen, Y., Li, Y., & Zhou, B Identification of the Roles of Coagulation-Related Signature and its Key Factor RABIF in Hepatoma Cell Malignancy, Recent patents on anti-cancer drug discovery. *Recent Pat Anticancer Drug Discov*. **19**, 695–710 (2024).
44. Sugo, M. et al. Syntaxin 17 regulates the localization and function of PGAM5 in mitochondrial division and mitophagy. *EMBO J.* **37**, e98899 (2018).
45. Chen, G. et al. A regulatory signaling loop comprising the PGAM5 phosphatase and CK2 controls receptor-mediated mitophagy. *Mol. cell* **54**, 362–377 (2014).
46. Zeb, A. et al. A novel role of KEAP1/PGAM5 complex: ROS sensor for inducing mitophagy. *Redox Biol.* **48**, 102186 (2021).
47. Drizyte-Miller, K., Chen, J., Cao, H., Schott, M. B. & McNiven, M. A. The small GTPase Rab32 resides on lysosomes to regulate mTORC1 signaling. *J. cell Sci.* **133**, jcs236661 (2020).
48. Seitz, S. et al. Hepatic Rab24 controls blood glucose homeostasis via improving mitochondrial plasticity. *Nat. Metab.* **1**, 1009–1026 (2019).
49. Wu, H. et al. Mitochondrial dysfunction promotes the transition of precursor to terminally exhausted T cells through HIF-1α-mediated glycolytic reprogramming. *Nat. Commun.* **14**, 6858 (2023).
50. Dang, B. et al. The glycolysis/HIF-1α axis defines the inflammatory role of IL-4-primed macrophages. *Cell Rep.* **42**, 112471 (2023).
51. Khan, T. G., Ginsburg, D. & Emmer, B. T. The small GTPase RAB10 regulates endosomal recycling of the LDL receptor and transferrin receptor in hepatocytes. *J. lipid Res.* **63**, 100248 (2022).
52. Li, Z. et al. Maturation of Lipophagic Organelles in Hepatocytes Is Dependent Upon a Rab10/Dynamin-2 Complex,. *Hepatology* **72**, 486–502 (2020).
53. Hamilton, M. C. et al. Systematic elucidation of genetic mechanisms underlying cholesterol uptake. *Cell Genom.* **3**, 100304 (2023).
54. Ladd, A., Duarte, S., Sahin, I. & Zarrinpar, A. Mechanisms of drug resistance in hepatocellular carcinoma. *Hepatology* **10**, 1097 (2023).
55. Hsu, C.-H., Huang, Y.-H., Lin, S.-M. & Hsu, C. AXL and MET in hepatocellular carcinoma: a systematic literature review. *Liver Cancer* **11**, 94–112 (2022).
56. Xu, J. et al. UBQLN1 mediates sorafenib resistance through regulating mitochondrial biogenesis and ROS homeostasis by targeting PGC1β in hepatocellular carcinoma. *Signal Transduct. Target. Ther.* **6**, 1–13 (2021).
57. Z. Ma, et al. Artesunate Sensitizes human hepatocellular carcinoma to sorafenib via exacerbating AFAP1L2-SRC-FUNDC1 axis-dependent mitophagy. *Autophagy* 1–16 (2023).
58. W. Wang, R. Zhang, N. Feng, L. Zhang, N. Liu, Overexpression of RBM34 Promotes Tumor Progression and Correlates with Poor Prognosis of Hepatocellular Carcinoma, Journal of Clinical and Translational Hepatology, (2022) 0-0.
59. Labun, K. et al. CHOPCHOP v3: expanding the CRISPR web toolbox beyond genome editing. *Nucleic Acids Res.* **47**, W171–W174 (2019).

Acknowledgements

The National Natural Science Foundation of China (Nos. 81972165 and 81972845) and Jiangsu Province Postgraduate Research and Practice Innovation Program Project (No. KYCX21_2667) provided funding for this study.

Author contributions

N Liu, L Zhang and J Zheng conceived the project. N Feng and R Zhang performed most of the experiments. W Wang, X Wen and N Zhang helped with the experiments and data collection. N Liu wrote the manuscript. All authors have read and discussed the manuscript.

Competing interests

The authors declare no competing interests.

Additional information

Supplementary information The online version contains supplementary material available at https://doi.org/10.1038/s42003-024-07028-1.

Correspondence and requests for materials should be addressed to Longzhen Zhang or Nianli Liu.

Peer review information *Communications Biology* thanks Karin Bartel and the other, anonymous, reviewers for their contribution to the peer review of this work. Primary Handling Editors: Georgios Giamas and Manuel Breuer.